AJBAR Vol. 3(2), April 2024: 103-118, ISSN: 2811-2881

Arid Zone Journal of Basic and Applied Research

Faculty of Science, Borno State University
Maiduguri, Nigeria

Journal homepage: https://www.azjournalbar.com

Research Article

Exploring the Antibacterial Properties of Hydrazone Schiff Bases Derived from 4-Aminodimethylbenzaldehyde: Synthesis, Characterization, and Activity Assessment

Grema A. Mala, Ibrahim M. Wakil, Hussaini Garba, Abubakar Mindia, Salihu A. Musa, Abubakar A. Ahmed, Mohammed B. Fugu, and Ibrahim Waziri*

[1]Department of Pure and Applied Chemistry, University of Maiduguri, P.M.B. 1069, Maiduguri, Borno State, Nigeria

***Corresponding author's Email**: triumph2236@gmail.com, doi.org/10.55639/607.313029

ARTICLE INFO:

Keywords:
Bacterial resistance,
Schiff base,
Hydrazones,
Structural activity relation

ABSTRACT

The urgent need for new antibiotics has fueled the synthesis and evaluation of organic molecules for their antibacterial activity. This study focuses on the synthesis of two hydrazone Schiff base compounds, (*E*)-*N*-(4-(dimethylamino)benzylidene)benzohydrazide (HSB1) and (*E*)-*N*-(4-(dimethylamino)benzylidene)-4-methylbenzohydrazide (HSB2). The compounds were synthesized through a condensation reaction between benzohydrazide, p-toluic hydrazide, and 4-aminodimethylbenzaldehyde in methanol solvent at room temperature, utilizing formic acid as a catalyst. The structures of the compounds were elucidated through comprehensive physicochemical and spectroscopic analyses, including elemental CHN-analysis, ^{1}H and ^{13}C NMR, FTIR, UV-Vis, and mass spectroscopies. These characterization techniques confirmed the successful formation of the compounds. The synthesized compounds were evaluated for their antibacterial activity, comparing them to the standard antibiotic ciprofloxacin. The *in vitro* disc diffusion method was employed to test the compounds against selected pathogenic bacteria, including Gram-positive strains, *Staphylococcus aureus* and *Streptococcus pyogenes*, as well as Gram-negative strains *Escherichia coli* and *Klebsiella pneumoniae*. The results demonstrated that the compounds exhibited concentration-dependent activity, with a preference for Gram-positive pathogens. Notably, HSB2 displayed superior antibacterial activity compared to HSB1. The study also postulated the structural activity relationship (SAR) and mode of action of the compounds. The SAR analysis suggested that the presence of specific chemical groups, such as aromatic rings and the hydrazone Schiff base moiety, contribute to their antibacterial activity.

Corresponding author: Ibrahim Waziri, **Email:** triumph2236@gmail.com
[1]Department of Pure and Applied Chemistry, University of Maiduguri, Borno State, Nigeria

INTRODUCTION

The emergence and spread of bacterial resistance to antibiotics have become a pressing global health concern (Uddin *et al.,*. 2021; Ayukekbong *et al.,*. 2017). Over the years, the misuse and overuse of antibiotics have led to the development of resistant bacterial strains, rendering many conventional antibiotics ineffective (Salam *et al.,*. 2023; Muteeb *et al.,*. 2023). This phenomenon, known as antibiotic resistance, poses a significant threat to public health as it reduces the efficacy of current treatment options and increases the morbidity and mortality rates associated with bacterial infections (Rossolini *et al.,*. 2014; Ventola, 2015; Church and McKillip, 2021). As a result, there is an urgent need to explore new sources of antimicrobial compounds that can effectively combat drug-resistant bacteria (Prestinaci *et al.,*. 2015; Ding *et al.,*. 2023).

In recent years, addressing the surge in bacterial resistance has become a major focus for researchers worldwide. One promising approach involves the identification and development of lead compounds with antibacterial properties (Chinemerem Nwobodo *et al.,*. 2022; McDowell *et al.,*. 2019). These lead compounds serve as starting points for the synthesis and optimization of novel antibacterial agents, offering a potential solution to overcome antibiotic resistance (Miethke *et al.,*. 2021; Breijyeh and Karaman, 2023). Various compounds have been investigated in this regard, including nanomaterials, coordination polymers, and coordination compounds. Among them, coordination compounds derived from hydrazone Schiff bases have emerged as promising candidates due to its dual functional groups (Santiago *et al.,*. 2020; Stojković *et al.,*. 2023).

Hydrazone Schiff bases possess additional therapeutic properties compared to other Schiff bases. This is attributed to the presence of an amide (-NHC=O-) functional group in addition to the azomethine (-C=N-) group (Elmacı *et al.,*. 2019). The combination of these functional groups enhances the biological activity of hydrazone Schiff bases, making them highly attractive for antibacterial applications (Elmacı *et al.,*. 2019).

Interestingly, in some cases, free hydrazone ligands have demonstrated greater biological viability than their corresponding complexes. This has sparked increased interest in exploring the utilization of uncoordinated hydrazone molecules rather than their complexes. Furthermore, the viability of free hydrazone ligands has garnered attention, potentially opening new avenues for the utilization of uncoordinated molecules in the quest for effective antibacterial (Yadav *et al.,*. 2023; Omidi and Kakanejadifard, 2020). They possess diverse chemical structures and exhibit a wide range of biological activities, including antibacterial properties. The hydrazone moiety enables these compounds to interact with bacterial targets and interfere with vital cellular processes, making them attractive candidates for combating drug-resistant bacteria (Omidi and Kakanejadifard, 2020; Popiołek, 2021).

Previous studies have reported on the antibacterial potential of hydrazone Schiff bases against various bacterial strains. For instance, Sharma *et al.* (2023) synthesized a series of hydrazone Schiff bases and evaluated their antibacterial activity against clinically relevant Gram-positive and Gram-negative bacteria. The results indicated significant antibacterial potential, demonstrating the effectiveness of hydrazone Schiff bases as antibacterial agents (Şenkardeş *et al.,*. 2023).

In another study, Adjissi *et al.* (2022) reported the synthesis and evaluation of hydrazone Schiff bases derived from different aromatic aldehydes against multidrug-resistant bacterial strains. The compounds exhibited notable antibacterial activity, suggesting their potential as lead compounds for developing new antibacterial agents (Adjissi *et al.,*. 2022). Similarly,

hydrazone derivatives derived from benzaldehyde were evaluated for anti-inflammatory activity, and result obtained shows a potent activity (Asim *et al.,*. 2012). These examples highlight the therapeutic properties of hydrazone Schiff bases and their potential as antibacterial agents. However, further exploration and investigation are necessary to expand the scope of their antibacterial activity and understand their mechanism of action against drug-resistant bacteria. Especially utilizing 4-aminodimethylbenzaldehyde, toluic hydrazide and benzohydrazide which are known to possess promising biological activities, including antibacterial, antioxidant, antimicrobial, antifungal, herbicidal, antiviral, and anti-inflammatory properties, making them versatile candidates for various therapeutic, pharmaceutical, and agricultural applications.

In this study, our aim is to explore the utilization of hydrazone Schiff bases derived from 4-aminodimethylbenzaldehyde as potential antibacterial agents. While previous studies have highlighted the antibacterial potential of hydrazone Schiff bases, our research contributes to the field by specifically investigating the antibacterial activity of these compounds derived from 4-aminodimethylbenzaldehyde. By evaluating their antibacterial potential and elucidating their mechanism of action, our study offers novel insights into the development of lead compounds with enhanced antibacterial properties. This research addresses the ongoing surge in bacterial resistance and provides valuable knowledge to guide the design and optimization of effective antibacterial agents.

2.0 EXPERIMENTAL

2.1. Reagents and physical measurements

The compounds were prepared by utilizing high-quality chemicals and reagents sourced from Sigma Aldrich. These chemicals were employed without additional purification. The chemicals include benzohydrazide, toluic hydrazide, 4-aminodimethylbenzaldehyde, methanol, ethanol, formic acid, and dimethyl sulfoxide. The synthesized compounds underwent characterization using standard physicochemical and spectroscopic techniques, including NMR (Nuclear Magnetic Resonance), FTIR (Fourier Transform Infrared Spectroscopy), UV (Ultraviolet-Visible Spectroscopy), MS (Mass Spectrometry), and CHN (Carbon-Hydrogen-Nitrogen) analysis.

2.2. Synthesis of the compounds

2.2.1. Synthesis of (*E*)-*N*-(4-(dimethylamino)benzylidene)benzohydrazide (HSB1)

This compound was synthesized by adopting our previously reported procedure after slight modification. 4-aminodimethylbenzaldehyde (0.6 g, 4.03 mmol, 1 eq) was dissolved in 20 mL of methanol and added to a stirring solution of benzohydrazide (1.2 g, 4.03 mmol, 1 eq) in 20 mL of methanol at room temperature. After complete addition, three to four drops of formic acid were added to the mixture while stirring to facilitate the condensation reaction. The stirring was continued at room temperature for four hours, and the precipitate was filtered using the gravity method, washed with methanol followed by ethyl ether to remove the unreacted products, and dried in a desiccator over fused calcium chloride. After drying, it was weighted, a percentage yield was estimated, and it was subsequently subjected to physicochemical and spectroscopic techniques for characterization. The reaction pathway is shown in **scheme 1**.

White solid; yield: (1.35 g, 83 %); m.p: 163 ^{o}C; ^{1}H NMR (500 MHz, DMSO-d_6): δ_H (ppm): 2.97 (s, 6H, $(CH_3)_2$), 6.76 (d, 2H, J = 8.5 Hz, Ar-H), 7.50 (d, 2H, J = 7.0 Hz, Ar-H), 7.52-7.55(t, 1H, J = 7.0 Hz, Ar-H), 7.88 (d, 2H, J = 7.5 Hz, Ar-H), 8.30 (s, 1H, HC=N), 11.53 (s, 1H, NH); ^{13}C NMR (125 MHz, DMSO-d_6): δ_C (ppm): 40.1 (CH_3), 111.1 (2C), 121.7, 127.6 (2C), 128.5 (2C), 131.5, 133.9, 148.8 (Ar-C), 151.7 (C=N), 162.8 (C=O); IR_{ATR} (ν_{max}/cm^{-1}): 2850 (C-H), 3300 (NH), 1720 (C=O), 1610 (C=N); UV-Vis (DMSO, 10^{-3} M,

nm): 278 ($\pi\rightarrow\pi^*$), 346 ($n\rightarrow\pi^*$); Anal. Calcd. (%) for $C_{16}H_{17}N_3O$ (267.1372): C, 71.81; N, 15.72; H, 6.41; Found: C, 71.78; N, 15.68; H, 6.40; MS (*m/z*): Calcd. = 290.1269 $[M+Na]^+$; Found = 290.1262 $[M+Na]^+$.

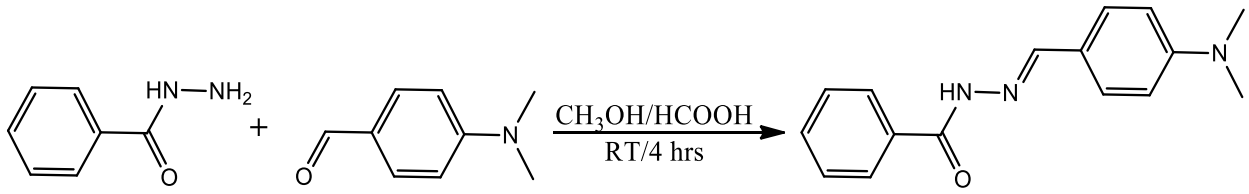

Scheme 1: Pathway for the synthesis of (*E*)-*N*-(4-(dimethylamino)benzylidene)benzohydrazide.

2.2.2. Synthesis of (*E*)-*N*-(4-(dimethylamino)benzylidene)-4-methylbenzohydrazide (HSB2).

The compound was synthesized following the procedure mentioned earlier, but with the substitution of benzohydrazide with toluic hydrazide. In summary, 4-aminodimethylbenzaldehyde (0.6 g, 4.03 mmol, 1 eq) was dissolved in 20 mL of methanol and added to a stirred solution of toluic hydrazide (0.61 g, 4.03 mmol, 1 eq) in 20 mL of methanol at room temperature. During stirring, three to four drops of formic acid were added to promote the condensation reaction. The mixture was stirred at room temperature for four hours, and the resulting precipitate was filtered using gravity filtration. The precipitate was then washed with methanol and subsequently with ethyl ether to remove any unreacted products. Afterward, the precipitate was dried in a desiccator containing fused calcium chloride, weighed, and the percentage yield was determined. The compound was further subjected to physicochemical and spectroscopic techniques for characterization. The reaction pathway is illustrated in **Scheme 2**.

Dark white solid; yield: (0.83 g, 78 %); m.p: 165 ^oC; ^1H NMR (500 MHz, DMSO-d_6): δ_H (ppm): 2.36 (S, 3H, CH_3), 2.95 (s, 6H, $(CH_3)_2$, 6.74 (d, 2H, *J* = 8.5 Hz, Ar-H), 7.30 (d, 2H, *J* = 7.5Hz, ar-H), 7.54 (d, 2H, *J* = 8.5 Hz, Ar-H), 7.82 (d, 2H, *J* = 7.5 Hz, Ar-H), 8.32 (s, 1H, HC=N), 11.49 (s, 1H, NH); ^{13}C NMR (125 MHz, DMSO-d_6): δ_C (ppm): 20.9 (CH_3), 48.6 $(CH_3)_2$, 111.7 (2C), 121.6 127.4, 128.3, 128.8, 130.8, 141.4, 148.4, 151.4 (Ar-C), 151.4 (C=N), 162.5 (C=O); IR_{ATR} (ν_{max}/cm^{-1}): 3200 (NH), 2800 (C-H), 1700 (C=O), 1600 (C=N); UV-Vis (DMSO, 10^{-3} M, nm): 264 ($\pi\rightarrow\pi^*$), 330 ($n\rightarrow\pi^*$); Anal. Calcd. (%) for $C_{17}H_{19}N_3O$ (281.1528): C, 72.57; N, 14.94; H, 6.81; Found: C, 72.53; N, 14.91; H, 6.80; MS (*m/z*): Calcd. = 282.1606 $[M+H]^+$; Found = 282.1604 $[M+H]^+$.

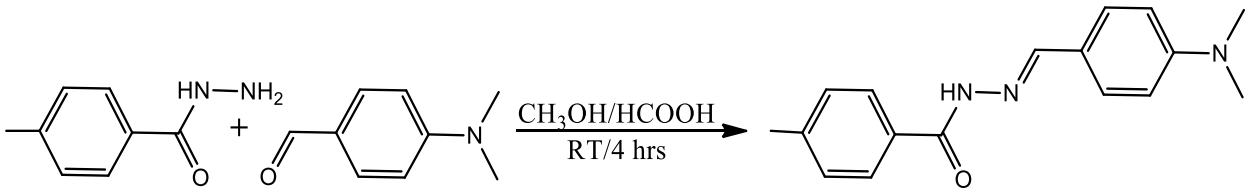

Scheme 2: Pathway for the synthesis of (*E*)-*N*-(4-(dimethylamino)benzylidene)-4-methylbenzohydrazide.

2.3. *In vitro* antimicrobial study

The antimicrobial activity of both control drugs and synthesized compounds was assessed using zone of inhibition studies. Gram-positive and gram-negative pathogenic strains, including *Staphylococcus aureus* (Sa), *Streptococcus*

pyogenes (Sp), *Escherichia coli* (Ec), and *Klebsiella pneumoniae* (Kp), were selected for the evaluation. These microorganisms are clinical isolates. the modified filter paper disc agar diffusion method (balouiri *et al.,*. 2016) was employed in this study. to perform the assay, a disc of blotting paper was impregnated with different concentrations of the standard and synthesized compounds at 10 and 20 µM/ml. subsequently, the disc was placed on a plate of sensitivity testing agar that had been uniformly inoculated with the respective bacterial strains. The plates were then incubated at 37 °C for 24 hours. following incubation, the diameter of the inhibition zone surrounding each disc was measured in millimeters using a transparent meter rule (khan *et al.,*. 2017). The experiment was conducted in triplicate, and the results were presented as the mean ± standard error of the mean (SEM).

3.0. RESULTS AND DISCUSSION

3.1. Synthesis and Physicochemical Properties

The schiff bases HBS1 and HBS2 were synthesized by a reaction between benzohydrazide, its methyl-derivative with 4-amino dimethyl benzaldehyde in solvent methanol and catalytic amount of formic acid (three drops). The resulting compounds were then dried and subjected to various characterization techniques including elemental analysis, FTIR, and ^{1}H and ^{13}C NMR spectroscopy. The FTIR spectra were obtained using an attenuated total reflectance (ATR) setup, while the NMR spectra were recorded in dimethyl sulfoxide (DMSO-d_6). The elemental analysis results for carbon (C), hydrogen (H), and nitrogen (N) were found to be in good agreement with the calculated values based on the proposed chemical formula. The agreement between the experimental and calculated elemental composition confirms the successful synthesis of the compounds. All the compounds were obtained in high yield, and isolated as white solid powder, stable in air and moisture. The melting point of the compounds was found to be within the range of 163–165 °C the sharp melting points observed for the synthesized compounds indicates their high purity and solid-state stability. Summary of the physicochemical properties of the compounds is given in table 1.

Table 1: Physicochemical properties of the compounds

Entry	Color	Yield (%)	m.p. (°C)	Elemental analysis: Calc. (Found)		
				C	H	N
HSB1	White	83	163	71.81(71.78)	6.41(6.40)	15.72(15.68)
HSB2	White	78	165	72.57(72.53)	6.81(6.80)	14.94(14.91)

3.2. Characterization

3.2.1. Nuclear magnetic resonance (NMR) spectroscopy

Nuclear Magnetic Resonance (NMR) spectroscopy plays a crucial role in the structural elucidation of organic molecules. It provides valuable information about the connectivity, stereochemistry, and chemical environment of atoms within a molecule (Emsley *et al.,*. 2013). To confirm the formation of the compounds and elucidate their structures, proton and carbon spectra were recorded in deuterated dimethyl sulfoxide (DMSO-d_6). The spectra obtained from this study are presented in Figure 1-2.

From these spectra, it is evident that HSB1 and HSB2 displayed six and eight peak signals,

respectively, accounting for all the protons in the compounds. Among these, the signal corresponding to the amide (NHC=O) moiety was observed at 11.54 and 11.49 ppm as a single peak in HSB1 and HSB2, respectively. In HSB2, the presence of a methyl substituent at the para position of one of the aromatic rings induces a subtle electronic effect on the neighboring amide group (Figure 2). The electron-donating nature of the methyl group slightly increases the electron density around the amide proton. Consequently, this electron-donating effect leads to a slight deshielding of the amide proton, causing it to be observed at a slightly lower chemical shift (up-field-shifted) compared to HSB1.

Similarly, the signal corresponding to the azomethine (HC=N) moiety was observed at 8.30 ppm in both HSB1 and HSB2 (Figures 1-2). The signal due to the azomethine protons appears in the up-field region of the spectra compared to the amide protons. This up-field shift is a result of the electron-withdrawing effect of the carbonyl group (C=O) due to the electronegative oxygen atom. The electron withdrawal decreases the electron density around the amide proton, leading to a downfield shift in the NMR spectrum.

Aromatic protons were found in the region of 6.73 to 7.90 ppm, accounting for all the protons within the molecules. Additionally, the terminal dimethyl protons were observed as a single peak at 2.96 ppm, integrating six protons. The up-field appearance of this proton in the spectra can be attributed to the electron density, proximity to the aromatic ring, and steric interaction effects. These factors result in a shielding effect on the proton, causing it to resonate at a higher field (upfield) in the spectrum.

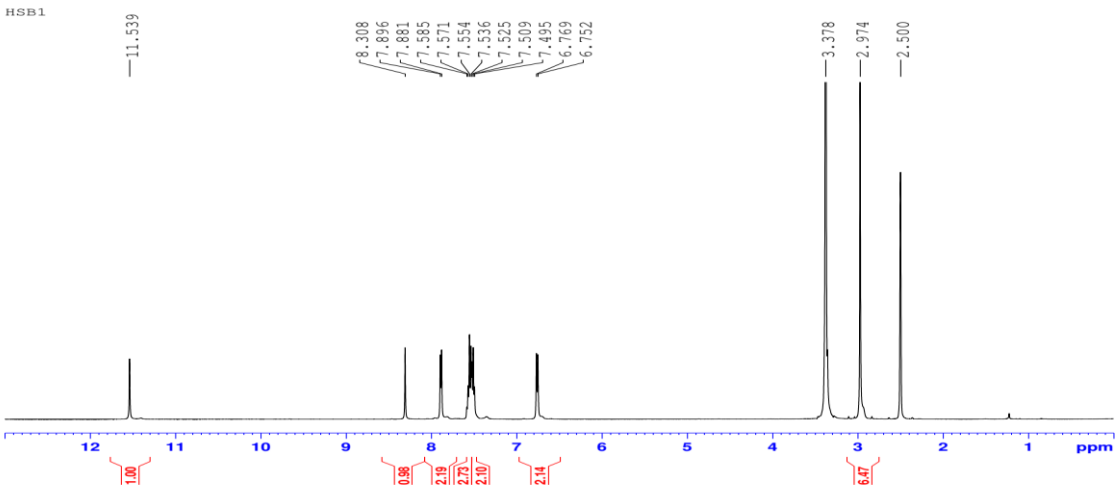

Figure 1: ^{1}H NMR spectrum of HSB1 (500 MHz, DMSO-d_6)

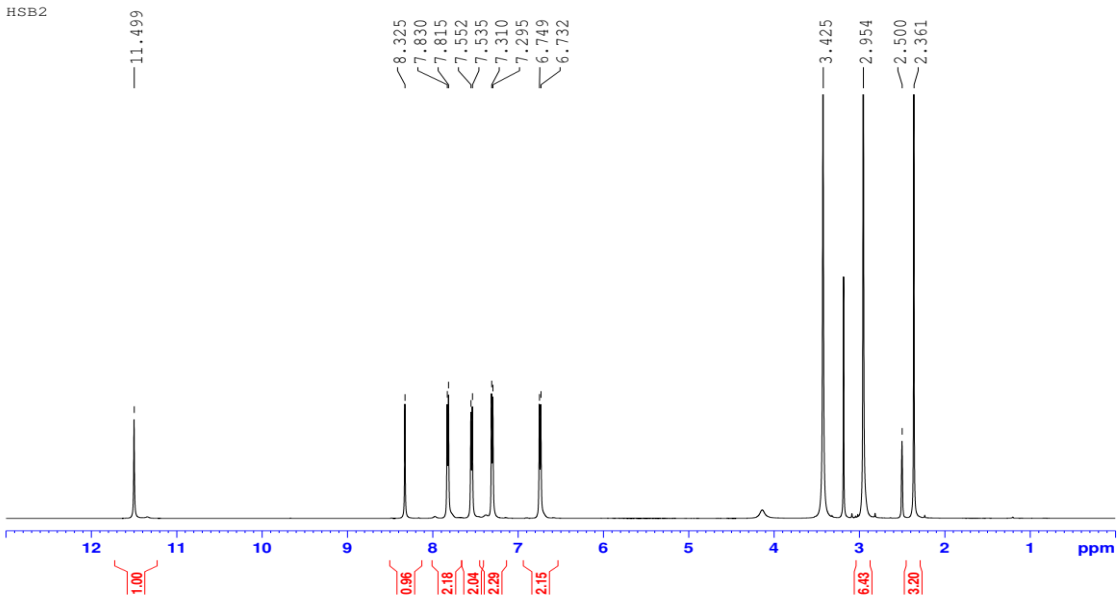

Figure 2: ^{1}H NMR spectrum of HSB2 (500 MHz, DMSO-d_6)

Furthermore, the carbon spectra of the compounds (Figures 3-4) exhibited characteristic signals corresponding to the carbon atoms within the compounds. Notably, the signal due to the amide (NHC=O) carbon peak appeared at 162.88 and 162.59 ppm in the spectra of HSB1 and HSB2, respectively (Figures 3-4). The slight differences in the chemical shifts of these carbons are attributed to the influence of the terminal methyl group in HSB2.

The signal due to the azomethine carbon in the compounds was observed at 148.88 and 148.46 ppm, respectively. Additionally, the carbon atom linking the aromatic ring with the terminal amino-methyl group was observed at 151.70 and 151.47 ppm in HSB1 and HSB2, respectively (Figures 3-4).

The data obtained from this study confirmed the successful isolation of the compounds, as the observed chemical shifts in the carbon and proton spectra matched the expected signals for the respective atoms within the compounds.

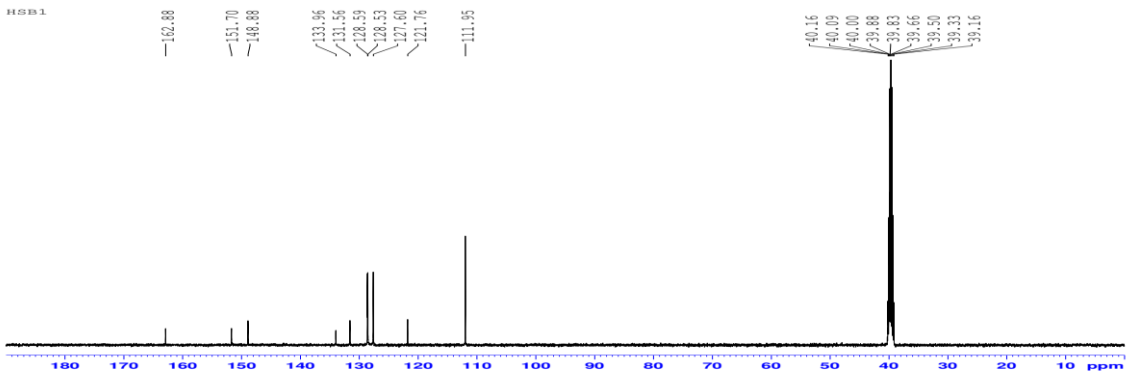

Figure 3: ^{13}C NMR spectrum of HSB1 (125 MHz, DMSO-d_6)

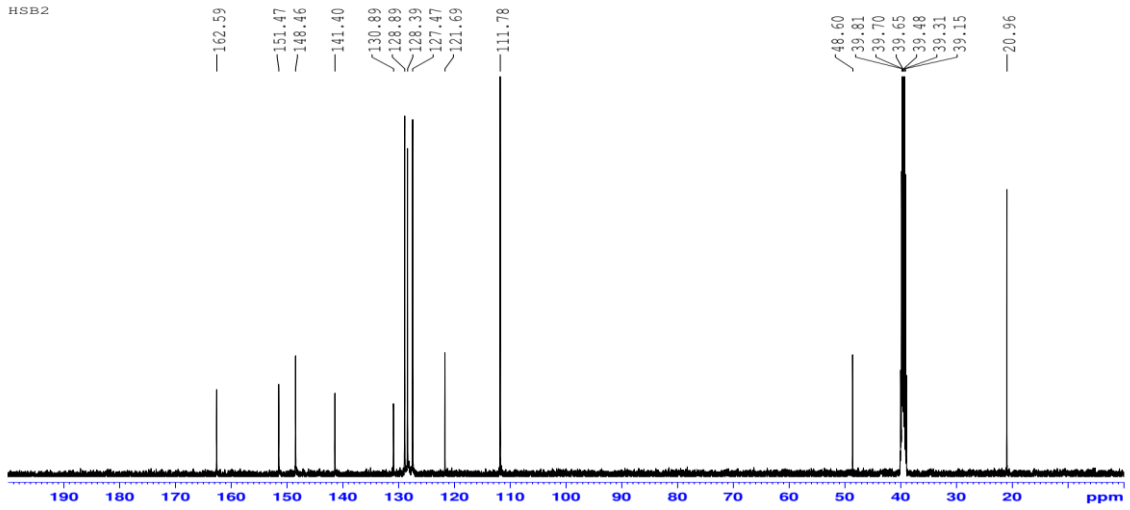

Figure 4: ^{13}C NMR spectrum of HSB2 (125 MHz, DMSO-d_6)

3.2.2. The Fourier-transform infrared (FTIR) spectroscopy

The FTIR spectra of HBS1 and HBS2 were recorded using an attenuated total reflectance (ATR) setup. These spectra contain valuable information about the functional groups present in the compounds, enabling structural characterization and identification of specific chemical bonds. The spectra were obtained in the range of 4000-500 cm^{-1} and the results obtained align with the expected values (Figures 5-6).

The compounds exhibit strong absorption peaks at 1638 and 1635 cm^{-1}, which are assigned to the (C=N) stretching vibration of the imine group (George *et al.*,. 2023), in HSB1 and HSB2, respectively (Figures 5-6). Additionally, the appearance of peaks at 3116 and 3170 cm^{-1}, assigned to NH stretching vibration bands (El-Mossalamy *et al.*,. 2024), confirms the formation of hydrazone Schiff bases. The infrared spectral data, combined with the NMR results, further confirms the successful formation of the compounds, and provides additional evidence supporting their structural characteristics

.

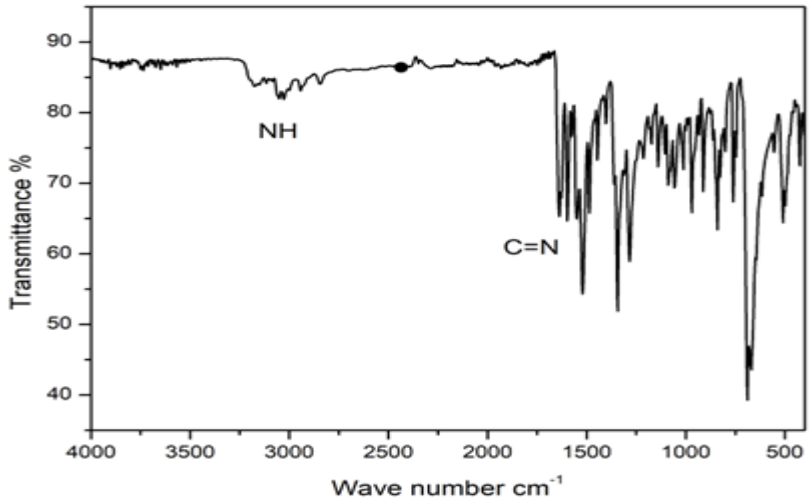

Figure 5: Infrared spectrum of HSB1

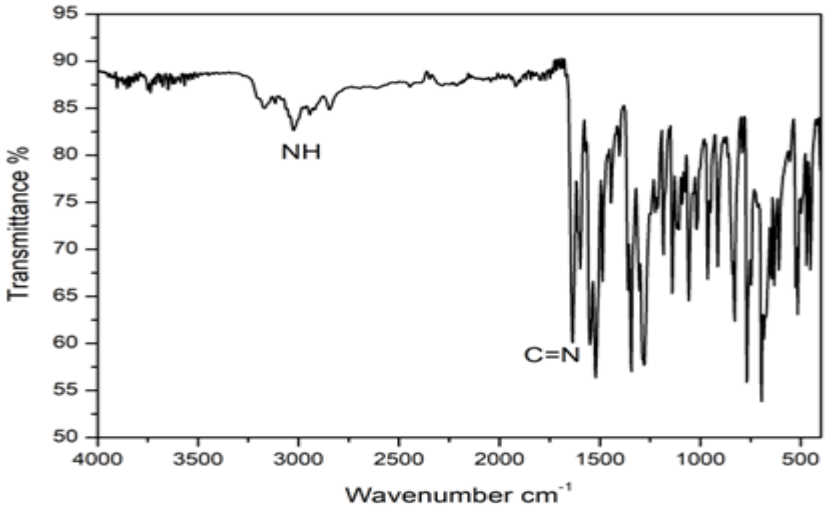

Figure 6: Infrared spectrum of HSB2

3.2.3. Ultraviolet Spectral Analysis

The UV-Visible absorption spectra of the compounds are utilized to investigate their electronic transitions and optical properties. This analysis provides insights into their potential applications in light-harvesting or as chromophores in various systems. In this study, the absorption spectra of the compounds HSB1 and HSB2 were obtained in the range of 250-800 nm, and the spectra are depicted in Figures 7-8.

From the spectra, it is evident that both compounds exhibit two absorption maxima each. HSB1 shows absorption peaks at approximately 265 nm and 342 nm, while HSB2 displays absorption peaks at around 283 nm and 313 nm. These absorption bands can be attributed to $\pi \rightarrow \pi^*$ transitions arising from the aromatic moieties and $n \rightarrow \pi^*$ transitions originating from the azomethine groups, respectively. These observations clearly demonstrate the electronic properties of the compounds and validate the presence of the expected functional groups.

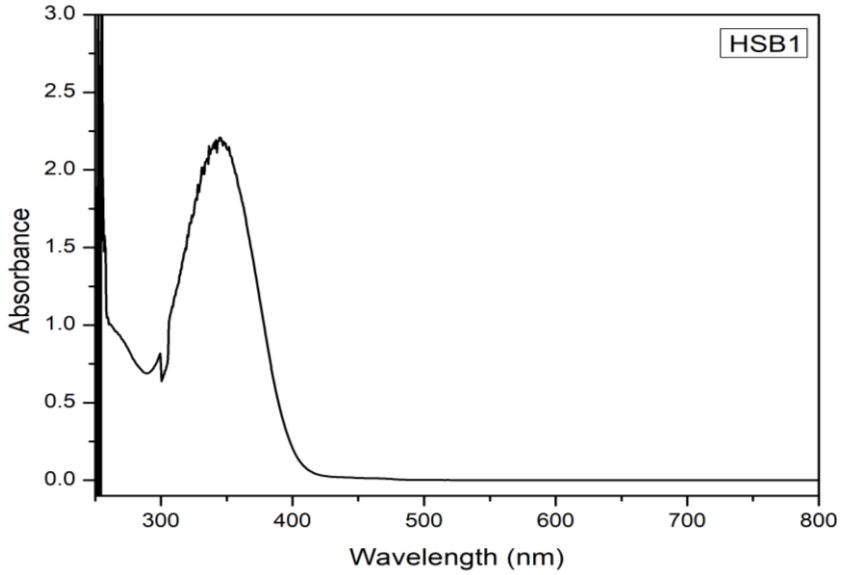

Figure 7: UV-Vis spectrum of HSB1

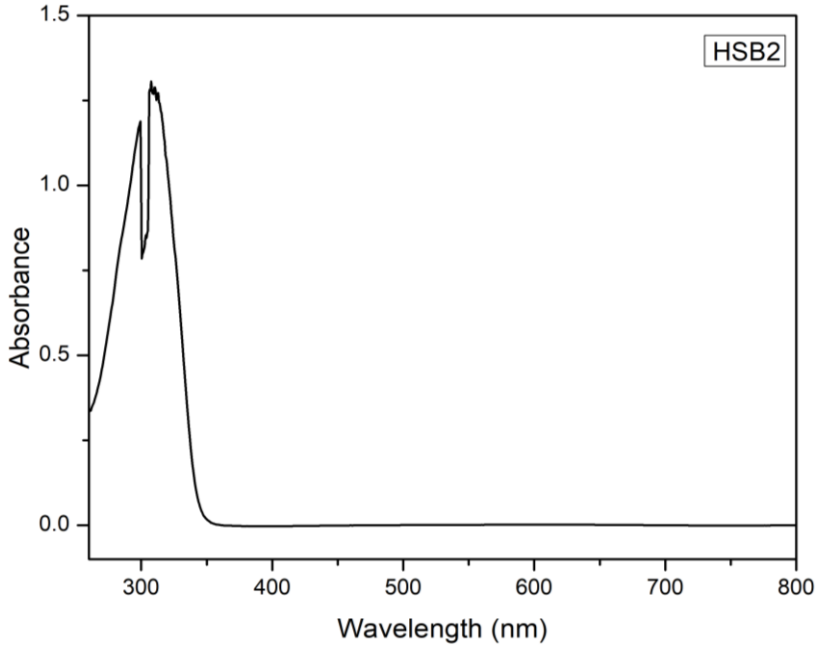

Figure 8: UV-Vis spectrum of HSB2

3.2.4. Mass spectroscopy

Mass spectrometry is an essential tool in structural elucidation, providing valuable information about the molecular mass, fragmentation patterns, and isotopic composition of compounds. It assists in determining molecular formulas, identifying functional groups, and characterizing chemical bonds. By ionizing and analyzing resulting ions, mass spectrometry reveals the connectivity and arrangement of atoms within a molecule, aiding in the determination of structural features. It serves as a powerful technique for compound identification and understanding their composition and structure (Ma, 2022).

In the context of the characterization and authentication of the compounds, mass spectrometry was utilized, and the spectra are presented in Figures 9-10. The compounds exhibit distinct m/z values that correspond well with the theoretical molecular weight of the compounds. In the spectrum of HSB1 (Figure 9), the observed m/z value is 290.1262, while the theoretical value is 290.1269, indicating the ionization of $[M+Na]^+$. Similarly, in the spectrum of HSB2 (Figure 10), the observed m/z value is 282.1604, and the theoretical value is 282.1606, representing the $[M+H]^+$ ionization mode. The mass spectrometry data strongly confirms the formation of the desired compounds (HSB1 and HSB2).

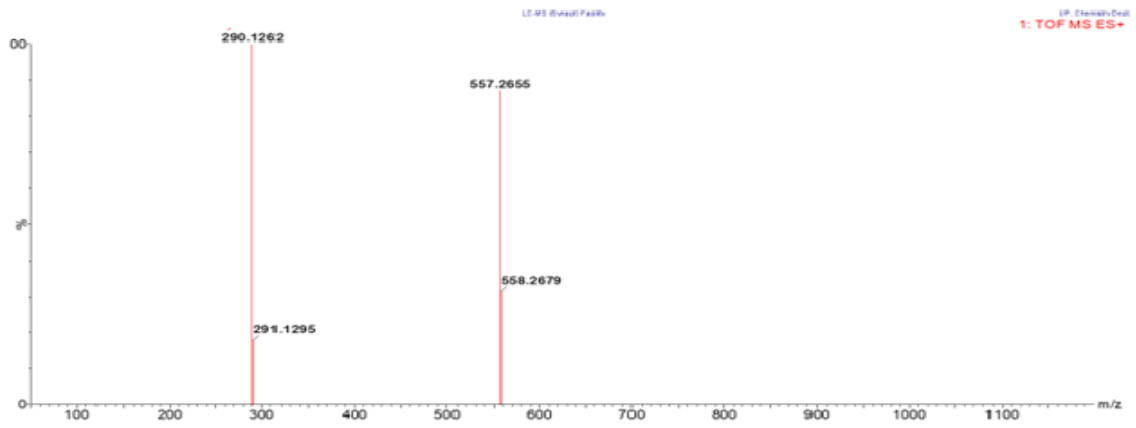

Figure 9: Mass spectrum of HSB1

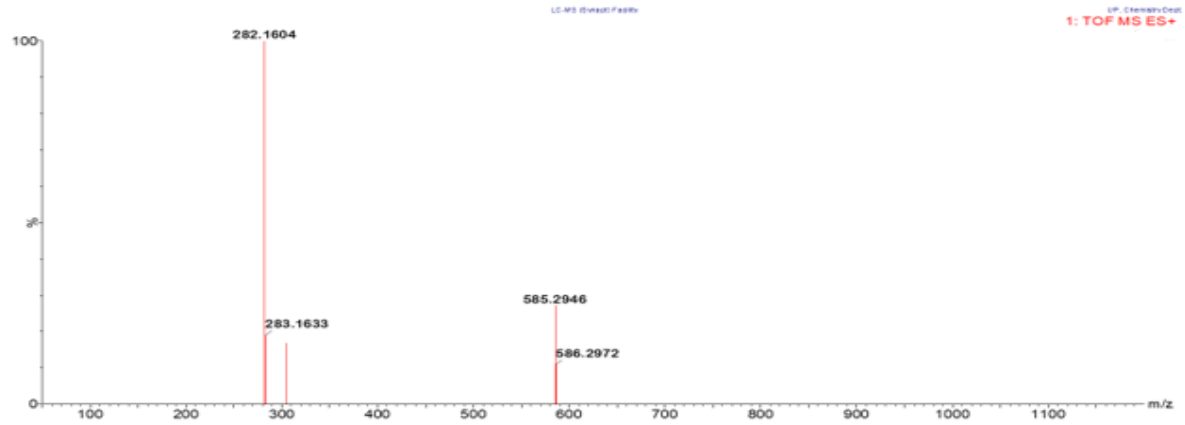

Figure 10: Mass spectrum of HSB2

3.3. Antibacterial Study

The synthesis and evaluation of organic molecules for antibacterial activity are motivated by the urgent need for new antibiotics, the opportunity to optimize their properties, the exploration of diverse chemical structures, and the potential for targeted interactions with bacterial targets. In this study, the synthesized compounds were assessed for their potential as antibacterial agents, comparing them to ciprofloxacin (used as a control) at concentrations of 10 and 20 µM. The evaluation was performed using a modified *in vitro* disc diffusion method, focusing on selected bacteria including Gram-positive strains *Staphylococcus aureus* (Sa) and *Streptococcus pyogenes* (Sp), as well as Gram-negative strains *Escherichia coli* (Ea) and *Klebsiella pneumoniae* (Kp) (Balouiri *et al.*,. 2016). Assessing the antibacterial activity of the synthesized compounds against these bacteria is highly relevant as it provides important insights into their potential for broad-spectrum activity, efficacy against multidrug-resistant strains, and their prospects as future antibacterial agents.

The findings of this study are presented in Figures 11-12. Overall, the compounds exhibited activity in a concentration-dependent manner. At a concentration of 10 µM, HSB1 showed zone of inhibition measurements of 8, 14, 5, and 6 mm against *Staphylococcus aureus* (Sa), *Streptococcus pyogenes* (Sp), *Escherichia coli* (Ec), and *Klebsiella pneumoniae* (Kb)

respectively. In comparison, HSB2 exhibited zones of inhibition measurements of 13, 19, 7, and 9 mm respectively on the same bacteria (Figure 11). Similarly, at a concentration of 20 µM, HSB1 demonstrated zone of inhibition measurements of 15, 18, 8, and 9 mm against Sa, Sp, Ec, and Kb respectively (Figure 12). At the same concentration, HSB2 exhibited zone of inhibition measurements of 17, 23, 12, and 11 mm respectively on Sa, Sp, Ec, and Kb (Figure 12). However, the control compound ciprofloxacin, at a concentration of 10 µM, displayed zone of inhibition measurements of 18, 21, 12, and 13 mm against Sa, Sp, Ec, and Kb respectively. At a concentration of 20 µM, the control showed zone of inhibition measurements of 22, 24, 15, and 16 mm on the same organisms respectively. These results indicate that none of the compounds surpassed the activity of the control on the tested bacteria. Moreover, HSB2 demonstrated higher activity compared to HSB1, and both compounds exhibited greater activity against Gram-positive bacteria compared to Gram-negative bacteria, suggesting a single spectrum of activity. The increased activity of HSB2 over HSB1 could be attributed to the presence of additional alkyl substituents at the para position on one of the aromatic rings in HSB2. The presence of an alkyl substituent in a compound has the potential to enhance antibacterial activity through improved membrane penetration, reduced susceptibility to efflux mechanisms, and modulation of interactions with intracellular targets (Qun *et al.*,. 2023).

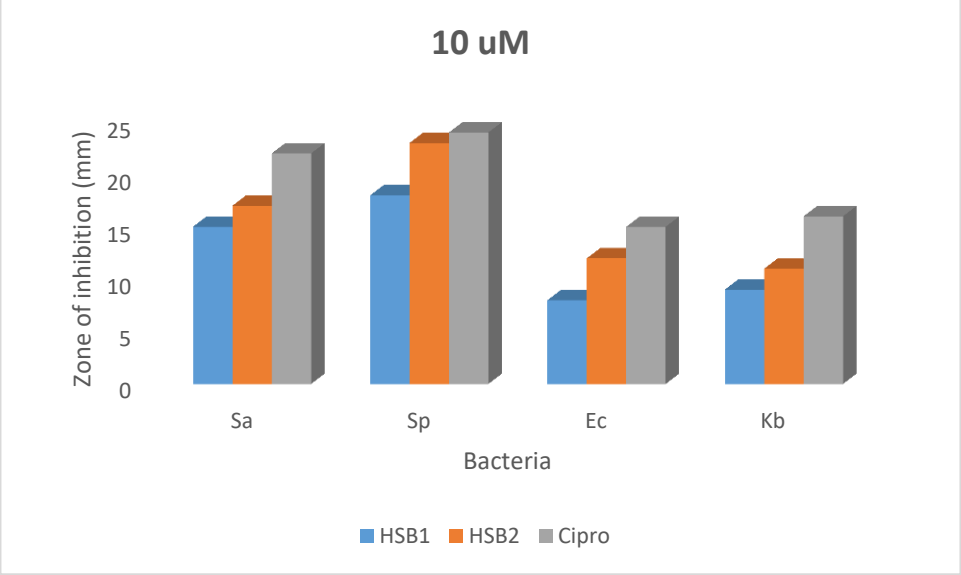

Figure 11: Antibacterial Activity of compounds comparative to ciprofloxacin at conc. of 10 µM

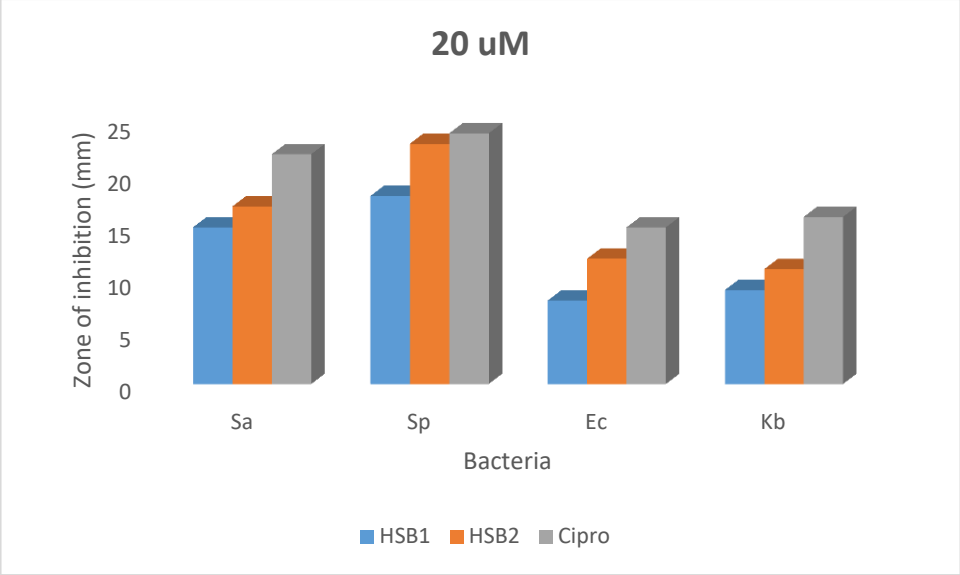

Figure 12: Antibacterial Activity of compounds comparative to ciprofloxacin at conc. of 20 µM

3.4. Structural Activity Relationship and Mode of Action

The structural activity relationship (SAR) and mode of action of the hydrazone Schiff bases (HSB1 and HSB2) can be described as follows:

3.4.1. Structural Activity Relationship (SAR)

1. Aromatic Rings: Both compounds, HSB1 and HSB2, contain two aromatic rings. The presence of aromatic rings in these compounds can contribute to their antibacterial activity by facilitating interactions with bacterial targets.
2. N-$(CH_3)_2$ Moiety: Both compounds feature an N-$(CH_3)_2$ (dimethyl amino) group attached to one end of the aromatic ring. This moiety can influence the compound's lipophilicity and enhance its membrane penetration, which can contribute to antibacterial activity.
3. Azomethine and Amide Groups: Both compounds possess a combination of azomethine (-N=CH-) and amide (-CONH-) functional groups. These groups can contribute to the compound's stability and potential interactions with bacterial targets, thereby influencing antibacterial activity.
4. Methyl Substituent: HSB2 contains an additional methyl substituent on its other aromatic ring. This methyl group can further modulate the compound's physicochemical properties, such as lipophilicity and steric effects, potentially enhancing its antibacterial activity.

3.4.2. Mode of Action

The exact mode of action of the hydrazone Schiff bases (HSB1 and HSB2) can be describe on the basis of their structural features as follows:

1. Target Interaction: The compounds' aromatic rings and functional groups can interact with specific bacterial targets, potentially interfering with essential cellular processes. This could involve binding to enzymes, receptors, or other biomolecules critical for bacterial growth and survival.
2. Membrane Disruption: The lipophilicity conferred by the N-$(CH_3)_2$ moiety and other structural features can enable the compounds to interact with bacterial cell membranes. They can disrupt membrane integrity, leading to leakage of cellular components or impairment of vital membrane functions.
3. Intracellular Effects: Once inside bacterial cells, the compounds can interfere with intracellular processes, such as nucleic acid synthesis, protein synthesis, or metabolic pathways. This disruption will impede bacterial growth and ultimately lead to cell death.

4.0. CONCLUSION

In this study, two hydrazone Schiff bases, HSB1 and HSB2, were successfully synthesized and characterized using physicochemical and spectroscopic techniques. The formation of the compounds was confirmed through rigorous analysis. The antibacterial activity of the synthesized compounds was evaluated against selected Gram-positive and Gram-negative bacteria. The results revealed a concentration-dependent activity, with HSB2 displaying superior activity compared to HSB1 against all tested bacteria. Furthermore, the compounds exhibited a greater level of activity against Gram-positive bacteria, such as *Staphylococcus aureus* and *Streptococcus pyogenes*, compared to Gram-negative bacteria like *Escherichia coli* and *Klebsiella pneumoniae*. This observation suggests a single spectrum activity, indicating a potential preference for targeting Gram-positive pathogens. The structural activity relationship (SAR) analysis indicated that the presence of aromatic rings, the N-$(CH_3)_2$ moiety, and the combination of azomethine and amide functional groups contribute to the antibacterial activity of the compounds. Additionally, HSB2 exhibited enhanced activity compared to HSB1, which may be attributed to the additional methyl substituent present in its aromatic ring. This structural modification potentially improved the compounds' physicochemical properties, leading to enhanced antibacterial effects.

Authorship Contribution statement

All authors contributed to the conception and design of the study, acquisition of data, analysis, and interpretation of results. They were all involved in drafting the manuscript and revising it critically for important intellectual content. All authors have given final approval for the version to be published.

Declaration of competing interest

The authors declare that there are no conflicts of interest regarding the publication of this manuscript**.**

Declaration of Funding

This research did not receive any specific funding.

Data Availability

The data that support this study are available in the article.

REFERENCES

Adjissi, L., N. Chafai, K. Benbouguerra, I. Kirouani, A. Hellal, H. Layaida, M. Elkolli, C. Bensouici, and S. Chafaa (2022). Synthesis, characterization, DFT, antioxidant, antibacterial, pharmacokinetics and inhibition of SARS-CoV-2 main protease of some heterocyclic hydrazones. *Journal of Molecular Structure* 1270:134005.

Asim Kaplancikli, Z., M. Dilek Altintop, A. Ozdemir, G. Turan-Zitouni, S. I Khan, and N. Tabanca (2012). Synthesis and biological evaluation of some hydrazone derivatives as anti-inflammatory agents. *Letters in Drug Design & Discovery* 9 (3):310-315.

Ayukekbong, J. A., M. Ntemgwa, and A. N. Atabe (2017). The threat of antimicrobial resistance in developing countries: causes and control strategies. *Antimicrobial Resistance & Infection Control* 6 (1):1-8.

Balouiri, M., M. Sadiki, and S. K. Ibnsouda (2016). Methods for in vitro evaluating antimicrobial activity: A review. *Journal of pharmaceutical analysis* 6 (2):71-79.

Breijyeh, Z., and R. Karaman (2023). Design and Synthesis of Novel Antimicrobial Agents. *Antibiotics* 12 (3):628.

Chinemerem Nwobodo, D., M. C. Ugwu, C. Oliseloke Anie, M. T. Al-Ouqaili, J. Chinedu Ikem, U. Victor Chigozie, and M. Saki (2022). Antibiotic resistance: The challenges and some emerging strategies for tackling a global menace. *Journal of clinical laboratory analysis* 36 (9):e24655.

Church, N. A., and J. L. McKillip (2021). Antibiotic resistance crisis: challenges

and imperatives. *Biologia* 76 (5):1535-1550.

Ding, D., B. Wang, X. Zhang, J. Zhang, H. Zhang, X. Liu, Z. Gao, and Z. Yu (2023). The spread of antibiotic resistance to humans and potential protection strategies. *Ecotoxicology and Environmental Safety* 254:114734.

El-Mossalamy, E., N. F. Al-Harby, S. A. Aal, N. Ali, M. El-Desawy, M. M. Elewa, and M. El Batouti (2024). Tenability on schiff base Hydrazone derivatives and Frontier molecular orbital. *Heliyon* 10 (2).

Elmacı, G., H. Duyar, B. Aydıner, I. Yahaya, N. Seferoğlu, E. Şahin, S. P. Çelik, L. Açık, and Z. Seferoğlu (2019). Novel benzildihydrazone based Schiff bases: Syntheses, characterization, thermal properties, theoretical DFT calculations and biological activity studies. *Journal of Molecular Structure* 1184:271-280.

Emsley, J. W., J. Feeney, and L. H. Sutcliffe (2013). *High Resolution Nuclear Magnetic Resonance Spectroscopy: Volume 2*. Vol. 2: Elsevier.

George, N., G. Singh, R. Singh, G. Singh, H. Singh, G. Kaur, and J. Singh (2023). Schiff base functionalized 1, 2, 3-triazole derivative for Fe (III) ion recognition, as N, O, O-Fe-O, O, N sandwich complex: DFT analysis. *Polyhedron* 242:116496.

Khan, S., M. Imran, M. Imran, and N. Pindari (2017). Antimicrobial activity of various ethanolic plant extracts against pathogenic multi drug resistant Candida spp. *Bioinformation* 13 (3):67.

Ma, X (2022). Recent advances in mass spectrometry-based structural elucidation techniques. *Molecules* 27 (19):6466.

McDowell, L. L., C. L. Quinn, J. A. Leeds, J. A. Silverman, and L. L. Silver (2019). Perspective on antibacterial lead identification challenges and the role of hypothesis-driven strategies. *SLAS DISCOVERY: Advancing Life Sciences R&D* 24 (4):440-456.

Miethke, M., M. Pieroni, T. Weber, M. Brönstrup, P. Hammann, L. Halby, P. B. Arimondo, P. Glaser, B. Aigle, and H. B. Bode (2021). Towards the sustainable discovery and development of new antibiotics. *Nature Reviews Chemistry* 5 (10):726-749.

Muteeb, G., M. T. Rehman, M. Shahwan, and M. Aatif (2023). Origin of Antibiotics and Antibiotic Resistance, and Their Impacts on Drug Development: A Narrative Review. *Pharmaceuticals* 16 (11):1615.

Omidi, S., and A. Kakanejadifard (2020). A review on biological activities of Schiff base, hydrazone, and oxime derivatives of curcumin. *RSC Advances* 10 (50):30186-30202.

Popiołek, Ł (202)1. Updated information on antimicrobial activity of hydrazide–hydrazones. *International Journal of Molecular Sciences* 22 (17):9389.

Prestinaci, F., P. Pezzotti, and A. Pantosti (2015). Antimicrobial resistance: a global multifaceted phenomenon. *Pathogens and global health* 109 (7):309-318.

Qun, T., T. Zhou, J. Hao, C. Wang, K. Zhang, J. Xu, X. Wang, and W. Zhou (2023). Antibacterial activities of anthraquinones: structure–activity relationships and action mechanisms. *RSC Medicinal Chemistry* 14 (8):1446-1471.

Rossolini, G. M., F. Arena, P. Pecile, and S. Pollini (2014). Update on the antibiotic resistance crisis. *Current opinion in pharmacology* 18:56-60.

Salam, M. A., M. Y. Al-Amin, M. T. Salam, J. S. Pawar, N. Akhter, A. A. Rabaan, and M. A. Alqumber (2023). Antimicrobial resistance: a growing serious threat for global public health. Paper read at Healthcare.

Santiago, P. H., C. M. Aiube, J. L. de Macedo, and C. C. Gatto (2020). Hydrazone-derived copper (II) coordination polymer as a selective liquid-phase catalyst: Synthesis, crystal structure and performance towards benzyl alcohol oxidation. *Molecular Catalysis* 496:111177.

Şenkardeş, S., D. Kart, B. Bebek, M. G. Gündüz, and Ş. G. Küçükgüzel (2023). Synthesis, antimicrobial properties and in silico studies of aryloxyacetic acid derivatives with hydrazone or thiazolidine-4-one scaffold. *Journal of Biomolecular*

Structure and Dynamics 41 (15):7421-7432.

Stojković, D., J. Petrović, T. Carević, M. Soković, and K. Liaras (2023). Synthetic and Semisynthetic Compounds as Antibacterials Targeting Virulence Traits in Resistant Strains: A Narrative Updated Review. *Antibiotics* 12 (6):963.

Uddin, T. M., A. J. Chakraborty, A. Khusro, B. R. M. Zidan, S. Mitra, T. B. Emran, K. Dhama, M. K. H. Ripon, M. Gajdács, and M. U. K. Sahibzada (2021). Antibiotic resistance in microbes: History, mechanisms, therapeutic strategies and future prospects. *Journal of infection and public health* 14 (12):1750-1766.

Ventola, C. L (2015). The antibiotic resistance crisis: part 1: causes and threats. *Pharmacy and therapeutics* 40 (4):277.

Yadav, A., C. Kaushik, and M. Kumar (2023). Hydrazones tethered disubstituted 1, 2, 3-triazoles: Design, synthesis, antitubercular and antimicrobial evaluation. *Journal of Molecular Structure* 1283:135163.